Transport properties of bismuth in non-quantizing magnetic fields: pseudo-parabolic variational calculation

1992 J. Phys.: Condens. Matter 4 1707

(http://iopscience.iop.org/0953-8984/4/7/009)

J. Phys.: Condens. Matter 4 (1992) 1707–1721. Printed in the UK

Transport properties of bismuth in non-quantizing magnetic fields: pseudo-parabolic variational calculation

I F I Mikhail and I M M Ismail
Department of Mathematics, Faculty of Science, Ain Shams University, Cairo, Egypt

Received 12 July 1990, in final form 13 May 1991

Abstract. The transport properties of bismuth are investigated within the pseudo-parabolic model by using a variational technique. The deformational potentials are accordingly taken to depend on the energy of electrons. The energy dependence considered is shown to be a general characteristic of the two-band model and is not confined to the case of bismuth. The convergence of the method is studied both numerically and analytically. Analytical expressions are obtained in the low-temperature range ($T < 77$ K) by using two variational parameters. For higher temperatures ($77\ \text{K} \leqslant T \leqslant 300$ K) the resistivity and thermoelectric power coefficients are calculated numerically to sufficiently high accuracy.

1. Introduction

The transport properties of the semimetal bismuth in the presence of a non-quantizing magnetic field have been studied by Mikhail *et al* [1], Hansen and Mikhail [2] and Gitsu *et al* [3]. In the first two references a so-called pseudo-parabolic model, which depends mainly on the Lax non-parabolic dispersion relation and a relaxation time having a specific energy dependence, has been utilized. In Gitsu *et al* [3] a variational technique has been employed to find the solution of the Boltzmann equation as a power series in energy. However, the convergence of their method deteriorated for non-parabolic dispersion and their results were thus obtained only for the parabolic case. It was pointed out in Hansen and Mikhail [2] that the deterioration in the results of Gitsu *et al* [3] may be due to their assumption concerning the energy dependence of the matrix element of electron–phonon interactions ($M_{\text{el-ph}}$). In their analysis this matrix element is taken to be independent of energy, unlike the case of the pseudo-parabolic model.

The primary aim of the present work is to calculate the transport tensors of bismuth by using a variational technique in which all the essential features of the pseudo-parabolic model are retained. Thus from the analytical point of view the basic differences between the present treatment and that of Gitsu *et al* [3] are in the form of the dispersion relation and in the energy dependence of $M_{\text{el-ph}}$. The dispersion relation is taken here to be non-parabolic and $M_{\text{el-ph}}$ is taken to depend on energy according to the result of Heremans and Hansen [4]. The energy dependence of the deformational potentials, which are the quantities that appear in the calculations, has been retrieved from the energy dependence of $M_{\text{el-ph}}$. These were taken to be independent of energy in Gitsu *et al* [3]. Also, as regards the numerical calculations, the temperature dependence of the deformational

0953-8984/92/071707 + 15 $04.50

potentials was obtained in Gitsu *et al* [3] by treating them as fitting parameters, and the masses of electrons and holes were taken to be independent of temperature. In the present calculations the whole set of input data of the pseudo-parabolic model (from Mikhail *et al* [1] and Hansen and Mikhail [2]) will be used after the convergence of the variational method is achieved.

It has further been shown analytically that three of the six quantities that determine the convergence of the method take fixed values, at any temperature, regardless of the number of variational parameters involved in the calculations. The convergence of the variational method would thus depend only on the convergence of the other three quantities. The convergence has, then, been studied numerically and has been found to be very fast, as we never used more than six terms of the power series to attain a sufficiently high accuracy.

Analytical expressions for the transport coefficients have also been obtained in the low-temperature range, where it is shown that the calculations can be performed satisfactorily by using two variational parameters. Most of the expressions obtained are found to agree with the corresponding results of the relaxation-time approximation [1, 4, 5]. Also, the expressions for the transport coefficients in zero magnetic field will be identical with those of the parabolic model if the Fermi energy is related to the parabolic Fermi energy in the usual manner. This is, in fact, one of the prime advantages of the pseudo-parabolic model [4]. The convergence of the method has also been investigated analytically in this temperature range. It is found that the method should converge whether the deformational potentials are taken to depend on energy according to the pseudo-parabolic model or to be energy-independent. It seems, therefore, that the energy dependence of $M_{\text{el-ph}}$ may not be the main reason for the deterioration of convergence in Gitsu *et al* [3], at least in the low-temperature range.

Some of the results have also been re-evaluated by using the parabolic dispersion relation and the same procedure used in Gitsu *et al* [3]. The motivation for such re-evaluation is to investigate the role of the off-diagonal deformational potential element, which was not taken into account by Gitsu *et al* [3, 6]. It is found that this element may have an appreciable effect.

The last motivation of the work is to investigate further the pseudo-parabolic energy dependence of the electron–phonon matrix element. In order to study the dependence, Heremans and Hansen [4] used an adjustable parameter. The value of this parameter was then retrieved from the experimental data of the zero-field thermoelectric power coefficients of bismuth. The result seems, therefore, to be restricted to the case of bismuth. It will, however, be shown in the present work (appendix 1) that the energy dependence of $M_{\text{el-ph}}$ obtained in [4] is valid, in general, for the Lax two-band model. It can thus be used for all group V semimetals and narrow-gap materials.

The present work is arranged in the following way. In section 2 the bases of the pseudo-parabolic variational technique and the general expressions for transport tensors are given. Analytical expressions for some of the basic quantities are derived in section 3. These expressions are valid at any temperature. The analytical study in the low-temperature range is performed in section 4, while the convergence of the method in this temperature range is investigated in section 4.1. The numerical calculations and results for $T \geqslant 77$ K are finally displayed in section 5.

2. Variational method and transport tensors

The distribution function for charge carriers (electrons and holes) may be expressed in the form

$$f_p = f_p^0 + (-\partial f_p^0/\partial E)\varphi_p \tag{1}$$

where $\boldsymbol{p}$ and E are the momentum and energy of an electron or a hole, f_p^0 is the Fermi–Dirac equilibrium distribution and φ_p is a measure for the deviation from equilibrium. Within the pseudo-parabolic model [4] the relation between E and $\boldsymbol{p}$ is given by the Lax non-parabolic dispersion relation:

$$\gamma(E) = E(1 + E/E_G) = \tfrac{1}{2}\boldsymbol{p}\mathbf{m}^{-1}\boldsymbol{p} \tag{2}$$

where $\mathbf{m}$ is the effective-mass tensor and E_G is the energy gap. Also, following Gitsu *et al* [3], φ_p may be expanded as

$$\varphi_p = \sum_i v_i \sum_{r=0}^{\infty} C_i^r (E/\theta_0)^r \tag{3}$$

where $\theta_0 = 1/k_B T$ and v_i are the components of the group velocity. In (3) C_i^r are variational parameters whose values can be obtained by substituting from (1) in the linearized Boltzmann equation of charge carriers [7] and applying the variational method in the presence of electric and magnetic fields [8, 9]. The solution should, of course, depend strongly on the form of the collision operator and the types of scattering mechanisms involved. In the present article it will be assumed, as has been consistently done in previous work, that the scattering of carriers is mainly due to interactions with acoustic phonons. In Gitsu *et al* [3, 6] the scattering term due to electron–phonon interactions has been expressed in terms of the elements D_{ij} of the deformational potential tensors of electrons and holes. These elements were taken in their work to be independent of energy for both non-parabolic and parabolic dispersions. It was felt at the beginning of this work that such an assumption may be the main reason for the deterioration of convergence in the numerical calculations of Gitsu *et al* [3] for non-parabolic dispersion. This, however, will be discussed in more detail in the following two sections.

In the present work the calculations are based on the pseudo-parabolic model. According to this model and the present calculations in appendix 1, the squared electron–phonon matrix element is taken to vary with energy as

$$M_{\text{el-ph}}^2 \propto (\gamma')^{-2} \qquad \gamma' = \mathrm{d}\gamma/\mathrm{d}E \tag{4}$$

rather than being constant. This will lead directly to deformational potential elements that depend on energy as $(\gamma')^{-1}$. We may thus take

$$D_{ij} = (\gamma')^{-1} D_{ij}^0 \tag{5}$$

where D_{ij}^0 is independent of energy. The results of Gitsu *et al* [3] would then be modified according to equation (5). The final expressions for the electrical and thermal currents $(\boldsymbol{J}, \boldsymbol{Q})$ and for the transport tensors of a single group of carriers are found to be

$$\boldsymbol{J} = \boldsymbol{\sigma}(\boldsymbol{B})\mathscr{E} - \boldsymbol{\theta}(\boldsymbol{B})\nabla_r T \tag{6a}$$

$$\boldsymbol{Q} = T\boldsymbol{\theta}(\boldsymbol{B})\mathscr{E} - \boldsymbol{\xi}(\boldsymbol{B})\nabla_r T \tag{6b}$$

and

$$\begin{aligned} \boldsymbol{\sigma}(\boldsymbol{B}) &= en(\boldsymbol{\mu}^{-1} + b_\sigma \mathbf{B})^{-1} \\ \boldsymbol{\theta}(\boldsymbol{B}) &= Sen(\boldsymbol{\mu}^{-1} + b_\theta \mathbf{B})^{-1} \\ \boldsymbol{\xi}(\boldsymbol{B}) &= Wen(\boldsymbol{\mu}^{-1} + b_\xi \mathbf{B})^{-1}. \end{aligned} \tag{7}$$

Here $\mathscr{E}$ and $\nabla_r T$ are the effective electric field and temperature gradient, $\boldsymbol{B}$ and $\mathbf{B}$ are

the magnetic field vector and antisymmetric tensor, e is the positive charge, and n is the density of carriers. Also

$$\begin{aligned}
&\boldsymbol{\mu} = (e/a)(\langle\sigma K\sigma\rangle/{}^0L_0^{3/2})\boldsymbol{\Gamma}^{-1} \\
&S = (k_B/Ze)\langle\sigma K\theta\rangle/\langle\sigma K\sigma\rangle \qquad W = (Tk_B^2/e^2)\langle\theta K\theta\rangle/\langle\sigma K\sigma\rangle \\
&b_\sigma = Z\,{}^0L_0^{3/2}/\langle\sigma B\sigma\rangle \qquad b_\theta = Z({}^0L_0^{3/2}/\langle\sigma K\sigma\rangle)\langle\sigma K\theta\rangle/\langle\sigma B\theta\rangle \\
&b_\xi = Z({}^0L_0^{3/2}/\langle\sigma K\sigma\rangle)\langle\theta K\theta\rangle/\langle\theta B\theta\rangle \qquad a = (6\theta_0^{3/2}/\pi\hbar^4)[(D_{11}^0)^2/c_{11}](2\det\mathbf{m})^{1/2} \\
&\langle\sigma K\sigma\rangle = \boldsymbol{L}_\sigma\mathbf{L}_K^{-1}\boldsymbol{L}_\sigma \qquad \langle\sigma B\theta\rangle = \boldsymbol{L}_\sigma\mathbf{L}_B^{-1}\boldsymbol{L}_\theta
\end{aligned} \tag{8}$$

with similar expressions for the other brackets $\langle\ldots\rangle$. Here, $Z = -1$ and $+1$ for electrons and holes respectively; c_{11} is a component of the elastic constant tensor while $\boldsymbol{\mu}$ stands for the mobility tensor; $\boldsymbol{\Gamma}$ is a tensor that is off-diagonal in the effective-mass frame and whose elements depend on the ratios $D_{22}/D_{11} = D_{22}^0/D_{11}^0$ and $D_{33}/D_{11} = D_{33}^0/D_{11}^0$. The forms of the elements of $\boldsymbol{\Gamma}$ are given in Gitsu *et al* [3]. Some modifications, however, are considered here in an appendix. Also, $\boldsymbol{L}_\sigma$ and $\boldsymbol{L}_\theta$ are either row or column vectors† while $\mathbf{L}_K$ and $\mathbf{L}_B$ are second-order symmetric tensors. The elements of $\boldsymbol{L}_\sigma$, $\boldsymbol{L}_\theta$, $\mathbf{L}_K$ and $\mathbf{L}_B$ are defined respectively by

$$\begin{aligned}
&(\boldsymbol{L}_\sigma)_s = {}^sL_{-1}^{3/2} \qquad (\boldsymbol{L}_\theta)_s = {}^{s+1}L_{-1}^{3/2} - \eta_F\,{}^sL_{-1}^{3/2} \qquad s = 0, 1, \ldots \\
&(\mathbf{L}_K)_{sr} = {}^{s+r}L_{-2}^2 \qquad (\mathbf{L}_B)_{sr} = {}^{s+r}L_{-2}^{3/2} \qquad s, r = 0, 1, \ldots
\end{aligned} \tag{9}$$

where

$${}^nL_k^m(\eta_F, \beta) = \int_0^\infty (-\partial f^0/\partial\eta)\eta^n(\eta + \beta\eta^2)^m(1 + 2\beta\eta)^k\,\mathrm{d}\eta \tag{10}$$

$\eta = E/\theta_0$, $\eta_F = E_F/\theta_0$, $\beta = \theta_0/E_G$ and E_F is the Fermi energy.

From the analytical point of view, the difference between the present results and those of Gitsu *et al* [3] is reflected in the definition of the tensor $\mathbf{L}_K$, which is defined in Gitsu *et al* [3] by

$$(\mathbf{L}_K)_{sr} = {}^{s+r}L_0^2 \qquad s, r = 0, 1, \ldots. \tag{11}$$

The differences in the numerical techniques and input data used in both treatments will be discussed in section 5.

Finally the same approach used in Hansen *et al* [5] can be employed to express the transport tensors (equation (7)) in the form

$$\boldsymbol{\sigma}(\boldsymbol{B}) = en[1 + b_\sigma^2 G(B^2)]^{-1}[\boldsymbol{\mu} - b_\sigma\boldsymbol{\mu}\mathbf{B}\boldsymbol{\mu} + b_\sigma^2\det(\boldsymbol{\mu})\boldsymbol{BB}] \tag{12a}$$

$$\boldsymbol{\theta}(\boldsymbol{B}) = Sen[1 + b_\theta^2 G(B^2)]^{-1}[\boldsymbol{\mu} - b_\theta\boldsymbol{\mu}\mathbf{B}\boldsymbol{\mu} + b_\theta^2\det(\boldsymbol{\mu})\boldsymbol{BB}] \tag{12b}$$

and

$$\boldsymbol{\xi}(\boldsymbol{B}) = Wen[1 + b_\xi^2 G(B^2)]^{-1}[\boldsymbol{\mu} - b_\xi\boldsymbol{\mu}\mathbf{B}\boldsymbol{\mu} + b_\xi^2\det(\boldsymbol{\mu})\boldsymbol{BB}] \tag{12c}$$

where

$$G(B^2) = \det(\mathbf{I} + \mathbf{B}\boldsymbol{\mu}) - 1. \tag{13}$$

Also, for weak magnetic fields equations (12*a*) and (12*b*) can be expressed in the form

$$\boldsymbol{\sigma}(\boldsymbol{B}) = en\{\boldsymbol{\mu} - b_\sigma\boldsymbol{\mu}\mathbf{B}\boldsymbol{\mu} + b_\sigma^2[\det(\boldsymbol{\mu})\boldsymbol{BB} - G(B^2)\boldsymbol{\mu}]\} \tag{14a}$$

and

$$\boldsymbol{\theta}(\boldsymbol{B}) = Sen\{\boldsymbol{\mu} - b_\theta\boldsymbol{\mu}\mathbf{B}\boldsymbol{\mu} + b_\theta^2[\det(\boldsymbol{\mu})\boldsymbol{BB} - G(B^2)\boldsymbol{\mu}]\}. \tag{14b}$$

† For simplicity the same symbol is used throughout for the vector and its transpose.

3. General analytical results

The convergence of the present variational method depends on the convergence of the six brackets $\langle \ldots \rangle$, which, in turn, determine the parameters b_σ, b_θ, b_ξ, S, W and the mobility tensor $\boldsymbol{\mu}$. General analytical expressions will be derived here for three of these brackets. These expressions are valid at any temperature and are independent of the number of variational parameters involved in the calculations. They can be obtained in the following way.

It is readily shown that the integrals ${}^nL_k^m$ satisfy the following recurrence relation for any k:

$$ {}^nL_k^m = {}^nL_{k-1}^m + 2\beta^{n+1}L_{k-1}^m. \tag{15}$$

Accordingly

$$ (\boldsymbol{L}_\sigma)_s = {}^sL_{-1}^{3/2} = {}^sL_{-2}^{3/2} + 2\beta^{s+1}L_{-2}^{3/2} \qquad s = 0, 1, \ldots . \tag{16}$$

In equation (16), $\boldsymbol{L}_\sigma$ is decomposed into two parts; the first is identical with the first row and first column of $\mathbf{L}_B$ while the second is proportional to the second row and second column of $\mathbf{L}_B$. Hence

$$ \langle \sigma B \sigma \rangle = \frac{1}{\det(\mathbf{L}_B)} \sum_{s,r} ({}^sL_{-2}^{3/2} + 2\beta^{s+1}L_{-2}^{3/2})(\mathrm{Co})_{rs}\, {}^rL_{-1}^{3/2} $$

$$ = \sum_r (\delta_{r0} + 2\beta\delta_{r1})\, {}^rL_{-1}^{3/2} = {}^0L_0^{3/2} \tag{17}$$

where $(\mathrm{Co})_{rs}$ is the cofactor of $\mathbf{L}_B$ corresponding to the element $(\mathbf{L}_B)_{rs}$ and equation (15) is used to obtain the last step. Similarly,

$$ \langle \sigma B \theta \rangle = {}^1L_0^{3/2} - \eta_F\, {}^0L_0^{3/2} = \int_0^\infty (-\partial f_0/\partial\eta)\bar{\gamma}^{3/2}(\eta - \eta_F)\, \mathrm{d}\eta \tag{18}$$

where $\bar{\gamma} = \gamma/\theta_0$. Also, by making use of (15), $\boldsymbol{L}_\theta$ can be decomposed in the same manner as in (16) and thus

$$ \langle \theta B \theta \rangle = {}^2L_0^{3/2} - 2\eta_F\, {}^1L_0^{3/2} + \eta_F^2\, {}^0L_0^{3/2} = \int_0^\infty (-\partial f_0/\partial\eta)\bar{\gamma}^{3/2}(\eta - \eta_F)^2\, \mathrm{d}\eta. \tag{19}$$

Furthermore, equation (17) implies that

$$ b_\sigma = Z \tag{20}$$

for any number of variational parameters. The results displayed in equations (17), (18), (19) and (20) are quite general. They do not depend on the energy dependence of the deformational potentials and are valid for both non-parabolic and parabolic† dispersions. These results have also been confirmed numerically. It seems that they have not been noticed by earlier workers [3]. In our opinion, this may be one of the main reasons for the deterioration of convergence of their results for non-parabolic dispersion.

In the pseudo-parabolic relaxation-time treatment [1], the coefficients equivalent to b_σ are equal to Z in the low-temperature range only. Accordingly, equation (12*a*) will

† The proof for parabolic dispersion is much simpler but the final results take the same form with $\bar{\gamma}$ being replaced by η.

be identical with the corresponding results of Mikhail *et al* [1] at low temperatures and will start to differ from them at high temperatures. Also, the expressions for the 12 weak-field galvanomagnetic coefficients of bismuth, which can be retrieved from (14*a*), will be equivalent to the standard expressions of Hartman [10] at all temperatures, unlike the case of the relaxation-time approximation.

4. Analytical calculations in the low-temperature range

The aim of the calculations in this section is to derive some analytical expressions within the variational approach which could be compared with the results obtained by using a relaxation-time technique [1, 4, 5]. In addition, these expressions would then be used to confirm the validity of the energy dependence of D_{ij}, which is displayed in equation (5), and to investigate analytically the convergence of the variational method.

In the low-temperature range the integrals ${}^nL_k^m$ can be performed by using the Bethe–Sommerfeld expansion. It can consequently be shown from equations (17), (18) and (19) that

$$\langle \sigma B \sigma \rangle = \tilde{\gamma}_F^{3/2} \qquad \langle \sigma B \theta \rangle = (\pi^2/2)\gamma_F' \tilde{\gamma}_F^{1/2} \qquad \langle \theta B \theta \rangle = (\pi^2/3)\tilde{\gamma}_F^{3/2} \tag{21}$$

where $\tilde{\gamma}_F = \tilde{\gamma}(E_F)$ and $\gamma_F' = \gamma'(E_F)$. As regards the three brackets $\langle \sigma K \sigma \rangle$, $\langle \sigma K \theta \rangle$ and $\langle \theta K \theta \rangle$, it has been found that the calculations with one variational parameter lead to unreasonable results, in contradiction to a remark made by Gitsu *et al* [3]. The calculations should thus be carried out with two variational parameters. Great care, however, must be taken when expanding the results in powers of $(k_B T/E_F)$ since most of the leading terms will be cancelled. It can be shown after a fair amount of manipulative algebra that

$$\langle \sigma K \sigma \rangle = \tilde{\gamma}_F \qquad \langle \sigma K \theta \rangle = (\pi^2/3)\gamma_F' \qquad \langle \theta K \theta \rangle = (\pi^2/3)\tilde{\gamma}_F. \tag{22}$$

Consequently we find by using equations (21) and (22) that

$$b_\xi = Z \qquad b_\theta = 2Z/3 \tag{23a}$$

$$\boldsymbol{\alpha}(\mathbf{0}) = S\mathbf{I} = \frac{k_B}{Ze}\frac{\pi^2}{3}\frac{k_B T}{E_F^*}\mathbf{I} \qquad W = TL_0 \tag{23b}$$

where $L_0 = (\pi^2/3)(k_B/e)^2$ is the Lorenz number, $\boldsymbol{\alpha}(\mathbf{0})$ is the thermoelectric power for a single group of carriers in zero magnetic field (partial Seebeck coefficient) and $E_F^* = \gamma_F/\gamma_F'$. The result obtained for $\boldsymbol{\alpha}(\mathbf{0})$ agrees with the corresponding result found by using the pseudo-parabolic relaxation time [4]. Moreover, it is readily shown that E_F^* stands for the corresponding parabolic Fermi energy. Accordingly, the numerical values of $\boldsymbol{\alpha}(\mathbf{0})$ for pseudo-parabolic and parabolic models will be identical. Also, the result obtained for W leads to an expression for the thermal conductivity that satisfies the Wiedemann–Franz law.

The comparison, in the low-temperature range, of equations (12*b*, *c*) and (14*b*) with the corresponding results† of Mikhail *et al* [1] shows that the value of b_ξ given in equation (23*a*) is identical with the value of the equivalent coefficient in Mikhail *et al* [1]. As regards the coefficient b_θ, it seems impossible to make a general analytical comparison.

† The corresponding expression for $\xi(B)$ is not given explicitly in Mikhail *et al* [1]. However, it can be easily obtained in a manner similar to that used in deriving equations (18*a*) and (18*b*) [1].

However, in the limit of weak magnetic field it can be shown that the equivalent value of b_θ in Mikhail *et al* [1] is $Z/2$ while the equivalent value of b_θ^2 is zero. Both of the two values do not agree with equation (23*a*). In view of this disagreement, the expressions for the 16 weak-field thermomagnetic coefficients of bismuth, which can be obtained from (14*b*), will not be identical with the results of Hansen *et al* [5].

It can thus be concluded that within the pseudo-parabolic model the differences that might occur at low temperatures between the results of the variational and relaxation-time methods will arise mainly due to the coefficient b_θ.

Finally, it may be of importance to rederive equations (23*a*) and (23*b*) by using deformational potential elements that are independent of energy. The results will correspond to the case considered in Gitsu *et al* [3]. It is found that the only coefficients that will be affected are those which depend on the bracket $\langle \sigma K \theta \rangle$. Accordingly, b_ξ and W take the same values as given in equations (23*a*) and (23*b*) while

$$\boldsymbol{\alpha}(\mathbf{0}) = S\mathbf{I} = (k_B/Ze)(\pi^2/3)(k_B T/\gamma_F \gamma_F')\mathbf{I} \qquad \text{and} \qquad b_\theta = \tfrac{8}{3} Z/(\gamma_F')^2. \tag{24}$$

It is readily shown that the result obtained above for $\boldsymbol{\alpha}(\mathbf{0})$ will be identical with the result of the relaxation-time approximation [5, 11] if the appropriate energy dependence of the relaxation time is taken ($\tau \propto \gamma^{-1/2}(\gamma')^{-1}$). The numerical values of $\boldsymbol{\alpha}(\mathbf{0})$, however, will differ substantially from the values of the parabolic model.

4.1. Convergence in the low-temperature range

In the first part of section 4 reasonable results have been obtained, at low temperatures, by using two variational parameters. Here, it will be shown that the addition of a third variational parameter will leave these results unaltered up to the first-order approximation in powers of $(k_B T/E_F)$. This in a sense means that the results converge in the low-temperature range to the expressions given in (22) and (23*a*, *b*). In order to show this, we consider the three brackets $\langle \sigma K \sigma \rangle$, $\langle \sigma K \theta \rangle$ and $\langle \theta K \theta \rangle$ and use the following formula, which depends on the partition of matrices [12]:

$$(X\mathbf{A}^{-1}Y)_{j+1} = (X\mathbf{A}^{-1}Y)_j + [x - (X\mathbf{A}^{-1}\boldsymbol{\Omega})_j][y - (Y\mathbf{A}^{-1}\boldsymbol{\Omega})_j][\omega - (\boldsymbol{\Omega}\mathbf{A}^{-1}\boldsymbol{\Omega})_j]^{-1} \tag{25}$$

where X and Y are either row or column vectors and $\mathbf{A}$ is a second-order symmetric tensor. The subscript j in $(X\mathbf{A}^{-1}Y)_j$ means that

$$X \equiv \{X_s, s = 0, 1, \ldots, j-1\} \qquad Y \equiv \{Y_s, s = 0, 1, \ldots, j-1\}$$

$$\mathbf{A} \equiv \{A_{rs}, s, r = 0, 1, \ldots, j-1\}.$$

Also,

$$\omega = A_{jj} \qquad x = X_j \qquad y = Y_j \qquad \boldsymbol{\Omega} = \{A_{jr}, r = 0, 1, \ldots, j-1\}.$$

If we now take $j = 2$ in equation (25) then $(X\mathbf{A}^{-1}Y)_{j+1}$ and $(X\mathbf{A}^{-1}Y)_j$ will represent one of the three brackets, being calculated respectively by using three and two variational parameters. The second term on the RHS of equation (25) will thus represent the correction due to the addition of the third variational parameter. For the three brackets it is found that the correction term can be neglected with respect to the term $(X\mathbf{A}^{-1}Y)_2$;

Table 1. Comparison between the order of the terms on the RHS of equation (25) for the three brackets $\langle \sigma K \sigma \rangle$, $\langle \sigma K \theta \rangle$ and $\langle \theta K \theta \rangle$ with $j = 2$. Each term is expressed as $R(k_B T/E_F)^s$ and the numbers in the table refer to s.

Bracket	$(\boldsymbol{XA}^{-1}\boldsymbol{Y})_2$	$\omega - (\boldsymbol{\Omega A}^{-1}\boldsymbol{\Omega})_2$	$x - (\boldsymbol{XA}^{-1}\boldsymbol{\Omega})_2$	$y - (\boldsymbol{YA}^{-1}\boldsymbol{\Omega})_2$	Correction term
$\langle \sigma K \sigma \rangle$	−1	−4	−3/2	−3/2	1
$\langle \sigma K \theta \rangle$	0	−4	−3/2	−1/2	2
$\langle \theta K \theta \rangle$	−1	−4	−1/2	−1/2	3

see table 1. Accordingly, $(\boldsymbol{XA}^{-1}\boldsymbol{Y})_3 \simeq (\boldsymbol{XA}^{-1}\boldsymbol{Y})_2$ and hence the results converge in this sense. The same conclusion is also found when the deformational potential elements are taken to be independent of energy. The results of Gitsu *et al* [3] may thus converge in the low-temperature range for non-parabolic dispersion.

5. Numerical calculations and results in the high-temperature range

At high temperatures ($T \geq 77$ K), the transport tensors of a single group of carriers can be calculated numerically from equation (12). The total transport tensors of bismuth can then be obtained by summing the contributions from its four groups of carriers. The resistivity and thermoelectric power tensors can finally be evaluated from the relations

$$\boldsymbol{\rho}(\boldsymbol{B}) = \boldsymbol{\sigma}^{-1}(\boldsymbol{B}) \qquad \text{and} \qquad \boldsymbol{\alpha}(\boldsymbol{B}) = \boldsymbol{\sigma}^{-1}(\boldsymbol{B})\boldsymbol{\theta}(\boldsymbol{B}) \tag{26}$$

where $\boldsymbol{\sigma}(\boldsymbol{B})$ and $\boldsymbol{\theta}(\boldsymbol{B})$ refer to the total tensors.

5.1. Non-parabolic dispersion, pseudo-parabolic model

As has been pointed out previously, the elements of the deformational potential tensor have been taken to be independent of energy in Gitsu *et al* [3]. However, they have considered the temperature dependence of these elements in the high-temperature range. For the elements D_{jj}^{e} and D_{jj}^{h} (e and h refer to electrons and holes), the temperature dependence has been retrieved from the experimental data of ρ_{33} and α_{11} in zero magnetic field. The ratios $(D_{22}/D_{11})^{e,h}$ and $(D_{33}/D_{11})^{e,h}$ have been assumed to be independent of temperature and equal to their values in the low-temperature range, which could be obtained from the measurements of Walther [13].

In the present analysis the deformational potentials are taken to depend on energy as given in equation (5). Thus, the temperature dependence of D_{jj}^{0e} and D_{jj}^{0h} cannot be obtained from the findings of Gitsu *et al* [3]. Moreover, the assumption that the ratio $(D_{22}^{0}/D_{11}^{0})^{e}$ is independent of temperature is certainly invalid for the pseudo-parabolic model where the scattering should increase rapidly with temperature along the bisectrix direction to compensate for the drastic decay of the mass element m_2^*. It has been readily shown in Mikhail and Ismail [14] that the scattering along this direction at $T = 300$ K should be higher by more than two orders of magnitude than its value at $T = 77$ K. In view of this, D_{jj}^{0e} and D_{22}^{0e} must be taken to vary independently with temperature in the case of the pseudo-parabolic model. Their values should then be obtained by treating them as independent adjustable parameters to fit the experimental data of weak-field

galvanomagnetic and thermomagnetic coefficients. This, however, seems to be very complicated since the dependence of these coefficients on the ratio D_{22}^{0e}/D_{11}^{0e} is through double integrals that determine the elements of Γ. In the present work a much simpler technique will be utilized. The only quantities that depend on the deformational potentials are the mobility elements of electrons and holes ($\mu = (e/a)\langle\sigma K\sigma\rangle/{}^0L_0^{3/2})\Gamma^{-1}$). Thus the variational procedure will be carried out until the brackets $\langle\sigma K\sigma\rangle$, $\langle\sigma K\theta\rangle$ and $\langle\theta K\theta\rangle$ converge to a sufficiently high accuracy. When convergence is achieved, the values of the mobility elements of electrons and holes will be taken from the results of Mikhail *et al* [1]†. So in the present calculations there is no need to find explicit values for the deformational potentials D_{ij}^0. However, the procedure employed is equivalent to choosing the values of these potentials (after the convergence is obtained) so that the mobilities of the pseudo-parabolic model are reproduced.

The input data for the present calculations are thus identical with those given in figure 1 and table 1 of [1] and in table 1 of [2]. The variational procedure is carried out in successive steps. In each step, an additional variational parameter is included. The procedure is performed until the maximum difference between the corresponding values of the brackets $\langle\sigma K\sigma\rangle$, $\langle\sigma K\theta\rangle$ and $\langle\theta K\theta\rangle$ in two successive steps is less than 1%. We never needed more than six variational parameters. The resistivity and thermoelectric power tensors are evaluated numerically as functions of the magnetic field for $T \geqslant 77$ K. The results are found to agree quantitatively with the results of the pseudo-parabolic relaxation-time model [1, 2] as well as with the experimental data reproduced in those two references. The results of some of the thermoelectric power coefficients are displayed in figures 1, 2 and 3. Also, the limiting behaviour in strong non-quantizing magnetic fields has been studied analytically, for all coefficients, by using equations (12*a*) and (12*b*). The results obtained agree entirely with those of the relaxation-time approximation [1, 2].

5.2. *Parabolic dispersion*

In spite of the fact that the main goal of the present numerical calculations is to evaluate the transport tensors for the pseudo-parabolic model, some of the results have been re-evaluated by using parabolic dispersion in order to investigate the following.

In Gitsu *et al* [3] the deformational potential tensor of electrons is taken to be diagonal in the mass frame of the principal ellipsoid. Walther [13], however, measured the elements of this tensor in the crystallographic frame at $T = 4.2$ K. Hansen [15] found that if the results of Walther are rotated to the mass frame they will still give an appreciable value to the off-diagonal element D_{23}^e. He pointed out further that this may be due to the large discrepancies in the measurements of Walther [13]. In a recent article by Lavrenyuk and Minina [16] the deformational potentials of bismuth have been measured in the crystallographic frame with relatively small discrepancies. The rotation of the new set of measurements leads to the same conclusion found by using the results of Walther [13]. This may confirm the importance of the role played by the off-diagonal element D_{23}^e. The effect of this term will thus be considered here. The expressions for the coefficients Σ_i, $i = 1, 2, 3$, which determine the elements of Γ should accordingly be modified to include the term D_{23}^e. Furthermore the expression for Σ_3 given in Gitsu *et al*

† The values of the mobility elements which could be obtained from the fitting of (14*a*) to the experimental results may differ from those reported in Mikhail *et al* [1], since $b_o = 1$. However, it seems reasonable to use the whole set of input data of the pseudo-parabolic model.

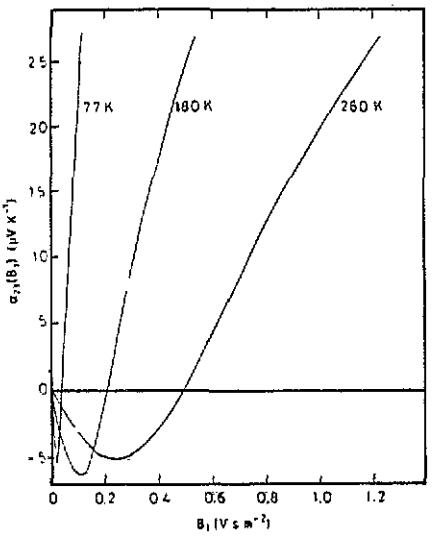

Figure 1. Graph of $\alpha_{23}(B_1)$ against the magnetic field B_1 at $T = 77$, 180, 260 K (pseudo-parabolic variational calculation). The corresponding pseudo-parabolic relaxation-time results and experimental data are given in figures 4*a*, *b* of Mikhail *et al* [1].

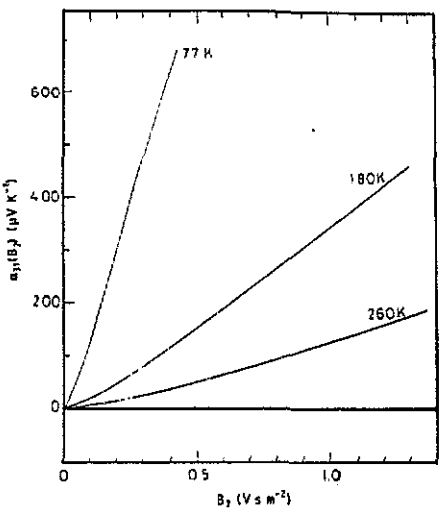

Figure 2. A plot of $\alpha_{31}(B_2)$ versus B_2 at $T = 77$, 180, 260 K, for the pseudo-parabolic variational calculation. The corresponding results of the relaxation-time approximation and experimental data are given in figures 7*a*, *b* of Mikhail *et al* [1].

[3] is found to be slightly in error (some signs are reversed). The modified expressions as well as the correct expression for Σ_3 are given in appendix 2 of the present article.

The elements of Γ should be calculated at first in the mass frame using the results given in Gitsu *et al* [3] and the modified expressions for Σ_i given in the appendix. The temperature dependences of D^e_{11} and D^h_{11} are taken to be identical with the results of Gitsu *et al* [3]. Also, the ratios D_{ij}/D_{11} are taken to be independent of temperature. Their values are thus taken from the results of Walther at $T = 4.2$ K. According to these results,

$$D^e_{11} = 2.2\,\text{eV} \qquad D^e_{22} = -6.13\,\text{eV} \qquad D^e_{33} = 1.93\,\text{eV} \qquad D^e_{23} = -0.677\,\text{eV}$$

in the mass frame of the principal electron ellipsoid and

$$D^h_{11} = D^h_{22} = -1.2\,\text{eV} \qquad D^h_{33} = 1.2\,\text{eV}$$

in the mass frame of the hole ellipsoid (the crystallographic frame). The mobility tensor of electrons obtained from equation (8) should finally (after the convergence is achieved) be rotated to the crystallographic frame. The effect of amending the incorrect signs in the expression for Σ_3 is found to be negligibly small both on the mobility elements as well as on the resistivity and thermoelectric power coefficients. On the other hand, appreciable changes have been noticed due to the consideration of the off-diagonal element D^e_{23}. As regards the mobilities of electrons, their relative ratios as well as their absolute values are improved so that they approach the corresponding data of the pseudo-parabolic model used in section 5.1. Also, in figure 4 the results obtained for the resistivity element $\rho_{11}(B_1)$ are given. It is readily shown from this figure that the relative deviation due to D^e_{23} in the saturation value of $\rho_{11}(B_1)$ is of the order of 6% at $T = 77$ K.

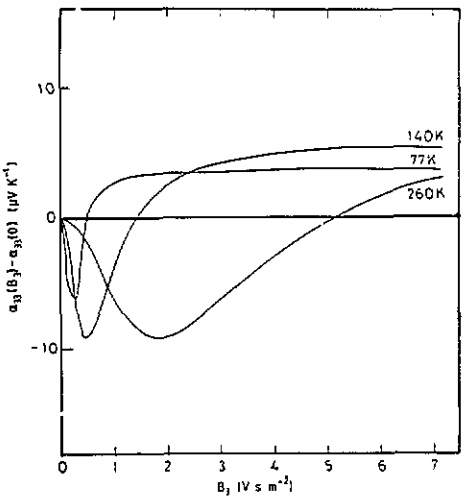

Figure 3. Graph of $\alpha_{33}(B_3) - \alpha_{33}(0)$ against B_3 at $T =$ 77, 140, 260 K (pseudo-parabolic variational calculation). The corresponding pseudo-parabolic relaxation-time results and experimental data are given in figures 9*a*, *b* of Mikhail *et al* [1].

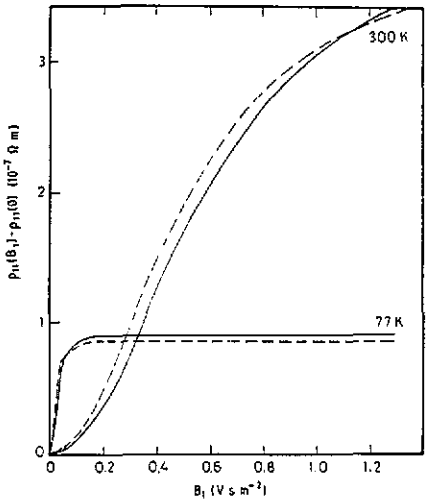

Figure 4. Graph of $\rho_{11}(B_1) - \rho_{11}(0)$ against B_1 at $T = 77$, 300 K for parabolic dispersion. The full and broken curves refer respectively to the case when the off-diagonal deformational potential D^S_{23} is taken into account and when its effect is neglected.

For $T = 300$ K, the maximum deviation in $\rho_{11}(B_1)$ is found to be 11% at $B_1 = 0.5$ T. The deviations in the other elements of $\boldsymbol{\rho}$ and $\boldsymbol{\alpha}$ are found to be of the same order.

6. Conclusions

The numerical results obtained for most of the resistivity and the thermoelectric power coefficients are in good quantitative agreement with the corresponding results of the relaxation-time approximation and with the experimental data. However, the comparison with the latter should only be considered below the Landau quantization limit. Also, the convergence of the method has been confirmed strongly, from both the analytical and numerical points of view. The energy dependence of the deformational potentials, within the pseudo-parabolic model, has given rise to results that are almost identical with the findings of the relaxation-time approximation. Moreover, it has been shown that the off-diagonal element of the deformational potential tensor may have a reasonable effect on the mobilities and transport coefficients.

Acknowledgments

We are greatly indebted to Dr O P Hansen for bringing to our attention the work of Gitsu *et al* and also pointing out that the off-diagonal component of the deformational potential tensor may be appreciable in the effective-mass frame. Also, I F I Mikhail wishes to express his appreciation for the hospitality of ICTP, Trieste, Italy, where a good part of the analytical calculations has been performed and the manuscript has been written.

Appendix 1. The energy dependence of the electron–phonon matrix element

Here, we show that the relation $M^2_{\text{el-ph}} \propto (\gamma')^{-2}$ is valid in general for the Lax two-band model. We first note that for the two-band model the parabolic Hamiltonian $\hat{H}_p$ is related to the non-parabolic Hamiltonian $\hat{H}$ by

$$\hat{H}_p = \hat{H}(1 + \hat{H}/E_G). \tag{A1.1}$$

If $\hat{H}$ is perturbed by $\hat{H}'$ then $\hat{H}_p$ will be perturbed by $\hat{H}'_p$, where

$$\hat{H}'_p = \hat{H}' + \hat{H}'(\hat{H}/E_G) + (\hat{H}/E_G)\hat{H}' + (\hat{H}')^2/E_G. \tag{A1.2}$$

The term $(\hat{H}')^2/E_G$ is a second-order term and can thus be dropped. Accordingly, the matrix elements due to a transition between two electron states of wavevectors $\boldsymbol{k}$ and $\boldsymbol{k}'$ are related by

$$\langle\psi_k|\hat{H}'_p|\psi_{k'}\rangle = (1 + E_{k'}/E_G + E_k/E_G)\langle\psi_k|\hat{H}'|\psi_{k'}\rangle \tag{A1.3}$$

where E_k and $E_{k'}$ are the eigenvalues of the unperturbed Hamiltonian $\hat{H}$ in the two states. The above relation is general for any perturbation $\hat{H}'$ not necessarily due to an electron–phonon interaction. For an electron–phonon interaction $E_k \simeq E_{k'}$, since the energy of phonons is much less than the energy of electrons. Hence,

$$\langle\psi_k|\hat{H}'|\psi_{k'}\rangle = \langle\psi_k|\hat{H}'_p|\psi_{k'}\rangle/\gamma' \qquad \gamma' = \mathrm{d}\gamma/\mathrm{d}E_k = 1 + 2E_k/E_G. \tag{A1.4}$$

This leads to the relation $M_{\text{el-ph}} = (M_p)_{\text{el-ph}}/\gamma'$, which, in turn, gives the required energy dependence of $M_{\text{el-ph}}$.

In the above derivation the same wavefunctions were used for both the parabolic and non-parabolic models. This is similar to the procedure used in Hansen [17] for the calculation of the velocity operator. In a more general treatment we may use the wavefunctions of the two-band model to find the non-parabolic electron–phonon matrix element. In this respect, we should note that $\hat{H}'_{\text{el-ph}}$ results mainly from the change of the crystal potential that occurs due to lattice vibrations. It may thus be supposed that $\hat{H}'$ is independent of electron spin and accordingly we may simplify the forms of two-band wavefunctions given in Mikhail and Ismail [14] to be

$$\psi_{kc} = [(E_{kc} + E_G)/(2E_{kc} + E_G)]^{1/2}(\psi_{k1} + [(\hbar\boldsymbol{k}\cdot\boldsymbol{t}^*)/(E_{kc} + E_G)]\psi_{k2}) \tag{A1.5a}$$

$$\psi_{kv} = [-E_{kv}/(-2E_{kv} - E_G)]^{1/2}(-[(\hbar\boldsymbol{k}\cdot\boldsymbol{t})/(-E_{kv})]\psi_{k1} + \psi_{k2}) \tag{A1.5b}$$

where

$$\psi_{kj} = \exp(\mathrm{i}\boldsymbol{k}\cdot\boldsymbol{r})u_j(\boldsymbol{r}) \qquad j = 1, 2 \qquad E_G\gamma(E_k) = \hbar^2(\boldsymbol{k}\cdot\boldsymbol{t})(\boldsymbol{k}\cdot\boldsymbol{t}^*)$$
$$\boldsymbol{t} = \langle u_1|\hat{\boldsymbol{p}}/m_0|u_2\rangle \qquad E_{kv} = -E_{kc} - E_G. \tag{A1.6}$$

In the above, c and v refer to the conduction and valence bands; $u_1(\boldsymbol{r})$ and $u_2(\boldsymbol{r})$ are the periodic wavefunctions at the bottom of the conduction band and the top of the valence band respectively; $\hat{p}$ is the momentum operator; and m_0 is the mass of a free electron. It is worthwhile noticing that $\hat{H}(1 + \hat{H}/E_G) = \tilde{\hat{H}}(1 + \tilde{\hat{H}}/E_G)$, where $\tilde{\hat{H}} = -\hat{H} - E_G$. A

perturbation of $\hat{H}$ by $\hat{H}'$ is therefore equivalent to a perturbation of $\hat{\bar{H}}$ by $\hat{\bar{H}}' = -\hat{H}'$. We may therefore have

$$\langle \psi_{kc} | \hat{H}' | \psi_{k'c} \rangle = \langle \psi_{kv} | \hat{\bar{H}}' | \psi_{k'v} \rangle. \tag{A1.7}$$

If we further take $E_k \simeq E_{k'}$ then equations (A1.7) and A(1.5a, b) give

$$\langle \psi_{k1} | \hat{H}' | \psi_{k'1} \rangle = -\langle \psi_{k2} | \hat{H}' | \psi_{k'2} \rangle. \tag{A1.8}$$

In the rest of the calculations we use only ψ_{kc}, since we are interested in intra-valley interactions. The suffix c will be dropped for simplicity. Equations (A1.3) and (A1.4) still hold, but $\langle \psi_k | \hat{H}'_p | \psi_{k'} \rangle$ will not represent directly the parabolic matrix element. By making use of equation (A1.5a) this element can be expressed as

$$\langle \psi_k | \hat{H}'_p | \psi_{k'} \rangle = \sum_{s,j=1}^{2} a_{sj} \langle \psi_{ks} | \hat{H}'_p | \psi_{k'j} \rangle. \tag{A1.9}$$

The coefficients a_{sj} can be obtained by direct substitution from (A1.5a). The matrix elements on the RHS of (A1.9) can be calculated by substituting from (A1.2) and using the relations

$$\hat{H}\psi_{k1} = \exp(i\boldsymbol{k}\cdot\boldsymbol{r})(\hbar/m_0)\boldsymbol{k}\cdot\hat{\boldsymbol{p}}u_1 \qquad \hat{H}\psi_{k2} = \exp(i\boldsymbol{k}\cdot\boldsymbol{r})[-E_G + (\hbar/m_0)\boldsymbol{k}\cdot\hat{\boldsymbol{p}}]u_2 \tag{A1.10}$$

together with similar relations for $\psi_{k'j}$, $j = 1, 2$. For example

$$\langle \psi_{k2} | \hat{H}'_p | \psi_{k'1} \rangle = (\hbar/m_0 E_G)\,[\langle u_2 | \exp(-i\boldsymbol{k}\cdot\boldsymbol{r})\hat{H}' \exp(i\boldsymbol{k}'\cdot\boldsymbol{r})\boldsymbol{k}'\cdot\hat{\boldsymbol{p}} | u_1 \rangle + \langle u_2 | \boldsymbol{k}\cdot\hat{\boldsymbol{p}} \exp(-i\boldsymbol{k}\cdot\boldsymbol{r})\hat{H}' \exp(i\boldsymbol{k}'\cdot\boldsymbol{r}) | u_1 \rangle]. \tag{A1.11}$$

In order to proceed we consider that $\{u_1, u_2\}$ is a complete set, which is one of the basic assumptions of the two-band model, and use the even and odd parities of u_1 and u_2. Accordingly

$$\langle \psi_{k2} | \hat{H}'_p | \psi_{k'1} \rangle = (\hbar/E_G)[\langle \psi_{k2} | \hat{H}' | \psi_{k'2} \rangle \boldsymbol{k}'\cdot\boldsymbol{t}^* + \boldsymbol{k}\cdot\boldsymbol{t}^* \langle \psi_{k1} | \hat{H}' | \psi_{k1} \rangle]. \tag{A1.12}$$

If we further take $E_k \simeq E_{k'}$ and use (A1.8) then $\langle \psi_{k2} | \hat{H}'_p | \psi_{k'1} \rangle = 0$. The other terms of (A1.9) can be calculated in the same manner. By making use of (A1.8) the final results are

$$\begin{aligned} &\langle \psi_{ks} | \hat{H}'_p | \psi_{k'j} \rangle = 0 \qquad \text{if } s \neq j \\ &\langle \psi_{k'1} | \hat{H}'_p | \psi_{k'1} \rangle = \langle \psi_{k2} | \hat{H}'_p | \psi_{k'2} \rangle. \end{aligned} \tag{A1.13}$$

The second equation in (A1.13) is expected since each of the two terms $\langle \psi_{kj} | \hat{H}'_p | \psi_{k'j} \rangle$, $j = 1, 2$, represents the parabolic matrix element with respect to a wavefunction of a single band. It is readily shown that the sum of the coefficients of these two terms in (A1.9) is equal to one if $E_k \simeq E_{k'}$. Hence

$$\langle \psi_k | \hat{H}'_p | \psi_{k'} \rangle = \langle \psi_{kp} | \hat{H}'_p | \psi_{k'p} \rangle \tag{A1.14}$$

where ψ_{kp} stands for a wavefunction of a single band, either ψ_{k1} or ψ_{k2}. Equation (A1.14) together with (A1.4) gives

$$\langle \psi_k | \hat{H}' | \psi_{k'} \rangle = \langle \psi_{kp} | \hat{H}'_p | \psi_{k'p} \rangle / \gamma' \tag{A1.15}$$

which yields the required relation between $M_{el\text{-}ph}$ and $(M_p)_{el\text{-}ph}$ and the required energy dependence of $M_{el\text{-}ph}$.

Appendix 2. Elements of the tensor Γ

The elements of the tensor Γ are given in Gitsu *et al* [3] in the form of double integrals over the polar and azimuthal angles (θ and φ) of the momentum–phonon space. These integrals depend on the quantities Σ_i, $i = 1, 2, 3$. As has been previously mentioned in section 5.2 the expressions for these quantities need to be modified to include the effect of the off-diagonal deformational potential D_{23}^{s}. The modified expressions take the form:

$$\Sigma_1^{1/2} = (\mathrm{RG})_1 + \frac{D_{23}}{D_{11}} C_\varphi S_\theta \left[-\alpha \left(\frac{m_2}{m_1}\right)^{1/2} S_\varphi S_\theta + \beta \left(\frac{m_3}{m_1}\right)^{1/2} C_\theta \right] \tag{A2.1}$$

$$\Sigma_2^{1/2} = (\mathrm{RG})_2 + \frac{D_{23}}{D_{11}} \left[\alpha\beta[1 - (1+r)^{1/2}] \left(\frac{m_2}{m_1} S_\varphi^2 S_\theta^2 + \frac{m_3}{m_1} C_\theta^2\right) + \left(\frac{m_2}{m_1}\right)^{1/2} \left(\frac{m_3}{m_1}\right)^{1/2} S_\varphi S_\theta C_\theta [1 + (1+r)^{1/2}] \right] \tag{A2.2}$$

$$\Sigma_3^{1/2} = (\mathrm{ARG})_3 + \frac{D_{23}}{D_{11}} \left\{ (1+r)^{1/2} C_\varphi^2 S_\theta^2 \left[\beta \left(\frac{m_2}{m_1}\right)^{1/2} S_\varphi S_\theta + \alpha \left(\frac{m_3}{m_1}\right)^{1/2} C_\theta \right] + \left(\frac{m_2}{m_1} S_\varphi^2 S_\theta^2 [\alpha^2 + \beta^2 (1+r)^{1/2}] - \frac{m_3}{m_1} C_\theta^2 [\beta^2 + \alpha^2 (1+r)^{1/2}] \right) \times \left[\beta \left(\frac{m_2}{m_1}\right)^{1/2} S_\varphi S_\theta - \alpha \left(\frac{m_3}{m_1}\right)^{1/2} C_\theta \right] \right\} \tag{A2.3}$$

where m_1, m_2, m_3 are the mass elements in the mass frame of reference, $S_\theta = \sin\theta$, $C_\theta = \cos\theta$, $S_\varphi = \sin\varphi$, $C_\varphi = \cos\varphi$, $\alpha = \sin\lambda$, $\beta = \cos\lambda$, $r = (c_{11} - c_{33})/(c_{33} - c_{44})$, λ is the tilt angle and c_{ij} are the elastic constants. Also, $(\mathrm{RG})_i$ stands for the corresponding results of Gitsu *et al* [3] while $(\mathrm{ARG})_3$ is the amended expression for Σ_3 without taking D_{23} into consideration and is given by

$$\begin{aligned}(\mathrm{ARG})_3 = {} & [(D_{22}/D_{11})(1+r)^{1/2} - 1](m_2/m_1)^{1/2} \alpha C_\varphi^2 S_\varphi S_\theta^3 \\ & + [(D_{33}/D_{11})(1+r)^{1/2} - 1](m_3/m_1)^{1/2} \beta C_\varphi^2 S_\theta^2 C_\theta \\ & + (D_{22}/D_{11})(m_2/m_1)^{3/2}[(1+r)^{1/2} - 1]\alpha\beta^2 S_\varphi^3 S_\theta^3 \\ & + (D_{33}/D_{11})(m_3/m_1)^{3/2}[(1+r)^{1/2} - \{1\}]\beta\alpha^2 C_\theta^3 \\ & + (m_2/m_1)(m_3/m_1)^{1/2} \beta S_\varphi^2 S_\theta^2 C_\theta ((D_{22}/D_{11})[\alpha^2 - \beta^2 \\ & - 2\alpha^2(1+r)^{1/2}] + (D_{33}/D_{11})[\beta^2(1+r)^{1/2} + \{\alpha^2\}]) \\ & + (m_3/m_1)(m_2/m_1)^{1/2} \alpha S_\varphi S_\theta C_\theta^2 ((D_{22}/D_{11})[\alpha^2(1+r)^{1/2} + \beta^2] \\ & + (D_{33}/D_{11})[\{\beta^2 - \alpha^2\} - 2(1+r)^{1/2}\beta^2]).\end{aligned} \tag{A2.4}$$

The above form differs from the corresponding result of Gitsu *et al* [3] in the terms between curly brackets $\{\ldots\}$. The signs of these terms have been reversed.

References

[1] Mikhail I F I, Hansen O P and Nielsen H 1980 *J. Phys. C: Solid State Phys.* **13** 1697

[2] Hansen O P and Mikhail I F I 1984 *Phys. Status Solidi* b **126** 721
[3] Gitsu D V, Golban I M and Kantser V G 1982 *Phys. Status Solidi* b **112** 473, **113** 59, **113** 497
[4] Heremans J and Hansen O P 1979 *J. Phys. C: Solid State Phys.* **12** 3483
[5] Hansen O P, Cheruvier E, Michenaud J-P and Issi J-P 1978 *J. Phys. C: Solid State Phys.* **11** 1825
[6] Gitsu D V, Golban I M and Kantser V G 1982 *Preprint* Kishinev (in Russian)
[7] Ziman J M 1960 *Electrons and Phonons* (Oxford: Clarendon)
[8] Garci-Moliner F and Simons S 1957 *Proc. Camb. Phil. Soc.* **53** 848
[9] Pinchuk I I and Tomchuk P M 1975 *Sov. Phys.–Semicond.* **9** 528 (*Fiz. Tekh. Poluprov.* **9** 801)
[10] Hartman R 1969 *Phys. Rev.* **181** 1070
[11] Hansen O P 1976 *J. Phys. C: Solid State Phys.* **9** 1457
[12] Mikhail I F I and Hanna I I 1973 *Ain Shams Sci. Bull.* **17** 321; Mikhail I F I 1971 *MSc Thesis* Ain Shams University, Cairo
[13] Walther K 1968 *Phys. Rev.* **174** 782
[14] Mikhail I F I and Ismail I M M 1986 *J. Phys. C: Solid State Phys.* **19** 5393
[15] Hansen O P private communications
[16] Lavrenyuk M Yu and Minina N Ya 1988 *Sov. J. Low Temp. Phys.* **14** 27 (*Fiz. Nizk. Temp.* **14** 52)
[17] Hansen O P 1981 *J. Phys. C: Solid State Phys.* **14** 5501